


Entrance surface dose measurements using a small OSL dosimeter with a computed tomography scanner having 320 rows of detectors

Kazuki Takegami^{1,6} · Hiroaki Hayashi²  · Kenji Yamada³ · Yoshiki Mihara⁴ · Natsumi Kimoto¹ · Yuki Kanazawa² · Kousaku Higashino^{2,3} · Kazuta Yamashita^{2,3} · Fumio Hayashi^{2,3} · Tohru Okazaki⁵ · Takuya Hashizume⁵ · Ikuo Kobayashi⁵

Received: 21 February 2016/Revised: 13 June 2016/Accepted: 14 June 2016/Published online: 24 June 2016
© Japanese Society of Radiological Technology and Japan Society of Medical Physics 2016

Abstract Entrance surface dose (ESD) measurements are important in X-ray computed tomography (CT) for examination, but in clinical settings it is difficult to measure ESDs because of a lack of suitable dosimeters. We focus on the capability of a small optically stimulated luminescence (OSL) dosimeter. The aim of this study is to propose a practical method for using an OSL dosimeter to measure the ESD when performing a CT examination. The small OSL dosimeter has an outer width of 10 mm; it is assumed that a partial dose may be measured because the slice thickness and helical pitch can be set to various values. To verify our method, we used a CT scanner having 320 rows of detectors and checked the consistencies of the ESDs measured using OSL dosimeters by comparing them with those measured using GafchromicTM films. The films were calibrated using an ionization chamber on the basis of half-value layer estimation. On the other hand, the OSL

dosimeter was appropriately calibrated using a practical calibration curve previously proposed by our group. The ESDs measured using the OSL dosimeters were in good agreement with the reference ESDs from the GafchromicTM films. Using these data, we also estimated the uncertainty of ESDs measured with small OSL dosimeters. We concluded that a small OSL dosimeter can be considered suitable for measuring the ESD with an uncertainty of 30 % during CT examinations in which pitch factors below 1.000 are applied.

Keywords OSL dosimeter · GafchromicTM film · Entrance surface dose · Computed tomography

1 Introduction

X-ray examinations using computed tomography (CT) and plain X-rays are widely used to diagnose various diseases in clinics, because of their simple and quick results. The X-ray equipment is properly controlled on the basis of several tests for accuracy using a management program; however, exposure doses for each patient are not measured because of a lack of detection systems. X-ray exposure has recently been increased [1] to obtain high-quality medical images for diagnosis. It is important for radiological technologists and medical doctors to optimize the balance between image quality and exposure doses to patients [2–4]. In particular, CT examinations result in higher X-ray exposure than plain X-ray examinations; thus, an increased risk of getting cancer has been noted [5]. It becomes imperative to construct a system to measure the exposure dose received during CT examinations. For clinical applications, the system should be easy to use.

✉ Hiroaki Hayashi
hayashi.hiroaki@tokushima-u.ac.jp

¹ Graduate School of Health Sciences, Tokushima University, 3-18-5 Kuramoto-cho, Tokushima, Tokushima 770-8503, Japan

² Graduate School of Biomedical Sciences, Tokushima University, 3-18-5 Kuramoto-cho, Tokushima, Tokushima 770-8503, Japan

³ Tokushima University Hospital, 3-18-5 Kuramoto-cho, Tokushima, Tokushima 770-8503, Japan

⁴ School of Health Sciences, Tokushima University, 3-18-5 Kuramoto-cho, Tokushima, Tokushima 770-8503, Japan

⁵ Nagase-Landauer, Ltd., C22-1 Suwa, Tsukuba, Ibaraki 300-2686, Japan

⁶ Present Address: Yamaguchi University Hospital, 1-1-1, Minamikogushi, Ube, Yamaguchi 755-8505, Japan

The exposure dose received during a CT examination is generally evaluated using the CT dose index (CTDI) method; however, it is difficult to evaluate the actual dose received by the patient [6]. Ideally, the organ doses of patients should be evaluated, but in reality only a few studies have estimated these, using several human body-type phantoms in which radiation detectors were implanted within the organs [7, 8]. Although this research method provides a good estimate, the systems are slightly complicated for application in clinical diagnosis. Using a suitable dosimeter, we plan to evaluate the doses not only of phantoms, but also of patients. At the beginning of our research, we focused on the entrance surface dose (ESD). The ESD is used for making practical evaluations; there is plenty of research concerning ESD measurements [8–15]. In this study, we used a small optically stimulated luminescence (OSL) dosimeter.

An OSL dosimeter called nanoDot™ was made commercially available by Landauer, Inc. The following useful characteristics of this dosimeter help us to measure the ESDs in the diagnostic X-ray region. First, the dosimeter is small and lightweight. The dosimeter will not interfere with X-ray examinations if patients wear the dosimeter on their bodies. Second, the nanoDot™ OSL dosimeter has a low detection efficiency. According to our previous studies [16–18], the nanoDot™ OSL dosimeter does not interfere with medical imaging in the diagnostic X-ray region; therefore, it is assumed that no additional artifacts appear on CT images. Third, the dosimeter can store the information regarding radiation detection for a long time and can be read many times without loss of information [18]; these characteristics play an important role in managing the ESD of each patient over the long term. Finally, compared with other radiation detectors, nanoDot™ OSL dosimeters are inexpensive; therefore, they can be produced in large quantities. To date, we have performed various basic studies on the use of the nanoDot™ OSL dosimeter in the diagnostic X-ray region such as an annealing device [19], evaluation of the uncertainty of the measurement system [18], angular dependence [20] and energy dependence [21]. Moreover, we proposed a practical dose calibration curve [22] in which the systematic uncertainty was evaluated to be 15 % by considering the angular dependence, energy dependence, and variability of individual dosimeters. In our system, the ESD and entrance skin dose can be derived from measured values without the need to gather information about the irradiation conditions, such as the tube voltages and incident X-ray angles. The nanoDot™ OSL dosimeter is expected to be suitable for direct measurements in clinical applications.

When performing CT examinations using collimated X-rays, the response of the nanoDot™ OSL dosimeter is unclear. Thus, we should evaluate the uncertainty of the

nanoDot™ OSL dosimeter when it is used for CT scans, where some dosimeters may be irradiated by the slit X-ray beam directly and the others may not. It is assumed that the responses of the dosimeter will change depending on the irradiation conditions, which are described as the slice thickness and helical pitch (pitch factor, PF). In contrast, for a cone beam CT system, there is no significant problem. Giaddui et al. reported that nanoDot™ OSL dosimeters can be used to measure doses with an accuracy of 6 % [23]. It is important for evaluating the ability to measure the ESD using the nanoDot™ OSL dosimeter in general CT systems.

The aim of this study is to evaluate the limitations and uncertainties when the nanoDot™ OSL dosimeter is used to measure the ESD during CT examinations.

2 Materials and methods

2.1 Dose measurement

2.1.1 Small OSL dosimeter: nanoDot™

We used a small OSL dosimeter called the nanoDot™ (Landauer, Glenwood, Illinois, USA) for measuring the ESDs. The size of the nanoDot™ OSL dosimeter is 10 mm in width, 10 mm in length, and 2 mm in thickness. The detector region is made of Al₂O₃:C. Information concerning X-ray exposure was measured using a reading device, the microStar® reader (Landauer, Glenwood, Illinois, USA), and was derived as countable values, which are referred to as counts. Before irradiation with X-rays, the nanoDot™ OSL dosimeter was sufficiently initialized [19]. The detection efficiency, ε , of nanoDot™ OSL dosimeters is incorporated into barcodes (ID). To account for the differences in ε , we used the values of counts/ ε [18–22].

To convert the counts/ ε values of the nanoDot™ OSL dosimeter to the ESD, a practical calibration curve developed in a previous study [22] was applied. Here, the ESD can be derived from the counts/ ε value as

$$ESD[\text{mGy}] = \frac{\text{Counts} - 240}{\varepsilon \cdot 3935}. \quad (1)$$

In our method, the nanoDot™ OSL dosimeter was calibrated using 83 kV X-rays [half-value layer (HVL) = 3.0 mmAl]. We proposed an adaptive 15 % uncertainty considering the effects of the angular dependence [20], energy dependence [21], variability of individual dosimeters [18], and a difference between mass energy absorption coefficients of air and soft-tissue. In the previous study [22], we reported that our calibration curve can convert counts/ ε to entrance skin dose, which is defined by the absorbed dose of the skin, e.g., soft-tissue. Although the ESD is defined by air

kerma, we can apply the previous curve to estimate the ESD; as described above, the effect of disregarding the difference between mass energy absorption coefficients of air and soft-tissue was considered in the uncertainty [see Eq. (2)]. A schematic drawing of our calibration is presented in Fig. 1. Here, we explain the method used to estimate the uncertainty. The total uncertainty of counts, σ_t , consists of the statistical uncertainty, σ_{sta} , and the systematic uncertainty, σ_{sys} , and their relationship is expressed as

$$\sigma_t = \sqrt{\sigma_{sta}^2 + \sigma_{sys}^2}, \quad (2)$$

where σ_{sys} in this analysis becomes 0.15 (15 %) [22]. In our experiments, the counts/ σ measured using the nanoDot™ OSL dosimeters were derived from an average of five consecutive readings [18]. Then, σ_{sta} is calculated as

$$\sigma_{sta} = \sqrt{\frac{\sum_i^5 \left(\frac{\sqrt{C_i/\varepsilon}}{C_i/\varepsilon} \right)^2}{5}}, \quad (3)$$

where C_i/ε is the counts/ ε value of the i th measurement.

2.1.2 Gafchromic™ film

We used a high-sensitivity Gafchromic™ film (XR-SP2, ASHLAND Ltd., New Jersey, USA) for measuring the profile of the ESD. This film can be used in the dose range of 0.5–50 mGy; the present experiments were performed in this range. To reduce contamination from natural radiation, new films were bought (lot number: 10261501, expiration date: October 2017), and the experiments were performed within 2 weeks. A flat panel scanner (Epson Expression 11000G flat-bed document scanner and DD-system, SEIKO EPSON Corporation, Suwa, Japan) combined with an analysis software (DD-Analysis Ver. 10.33, R-Tech Inc., Azumino, Japan) was used for reading the film density.

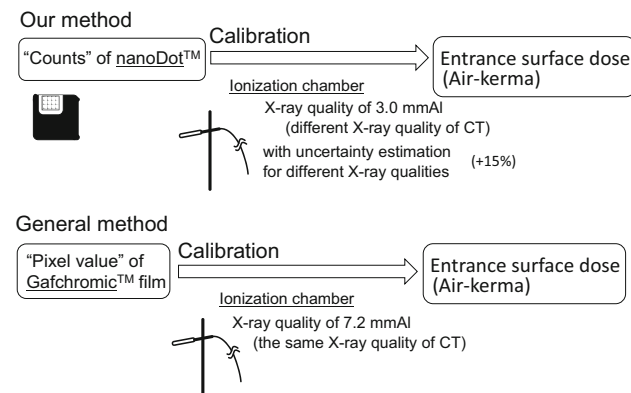


Fig. 1 Comparison of the calibrations of the nanoDot™ OSL dosimeter and the Gafchromic™ film

The Gafchromic™ film was well calibrated according to the general method [12, 24], as shown in Fig. 1. The quality of the radiation at the center axis of the CT X-rays (120 kV) was determined using a 0.6-cc Farmer-type ionization chamber (10X6-0.6CT, Radical Corporation, California, USA) connected to a dosimeter (Accu-Pro, Radical Corporation, California, USA). In the present experiment, the HVL was determined to be 7.2 mm. Then, using diagnostic X-ray equipment (Digital Diagnost, Koninklijke Philips N.V., Amsterdam, Netherlands), in which the same quality of radiation as that of a CT scanner was reconstructed, the measured value of the Gafchromic™ film was calibrated using the air kerma that was measured using the ionization chamber.

We checked the repeatability of the dose measurement system using a flat panel scanner. This system was remarkably stable, and the uncertainty of the repeatability of the system was estimated to be less than 0.5 %. Therefore, in this study, we did not consider the uncertainty of the dose measured with the Gafchromic™ film. On the other hand, the uncertainty of the calibration of the Gafchromic™ film was approximately 5 % owing to that of the ionization chamber. This uncertainty is not essential for our analysis, because the ionization chambers used in our experiments were calibrated by the same calibration field.

2.2 Experiments

Experiments were performed using a multidetector CT scanner (Aquilion ONE™, Toshiba Medical Systems, Otawara, Japan). The CT equipment has 320 rows of detectors that detect X-rays within a maximum range of 160 mm.

Figure 2 shows the experimental settings for X-ray irradiation in CT scans. A water phantom (conforming to JIS Z4915-1973; length = 45 cm, width = 30 cm, height = 20 cm) was placed on the scanning bed. Then, the center of the phantom was aligned with the isocenter of the CT

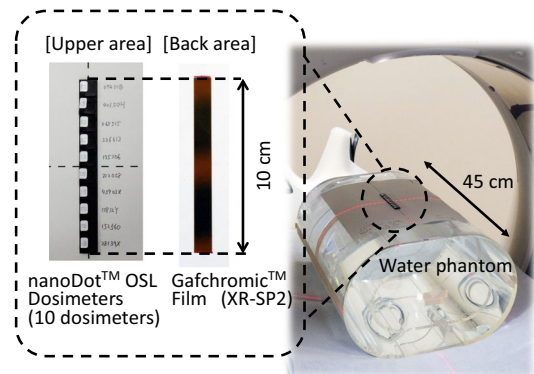


Fig. 2 Experimental setup for irradiating the nanoDot™ OSL dosimeters and the Gafchromic™ film. The dosimeters and film were placed on a water phantom

Table 1 Irradiation conditions in the CT scans

Detector rows	Tube current (mA)	Effective dose (mAs)	Helical pitch	Pitch factor
16	280	203	11	0.688
	380	202	15	0.938
	580	201	23	1.438
32	260	198	21	0.656
	340	201	27	0.844
	570	202	45	1.406
64	260	202	41	0.641
	330	199	53	0.828
	600	202	95	1.484
80	260	203	51	0.637
	330	203	65	0.813
	550	198	111	1.388
100	330	203	81	0.810
	560	201	139	1.390
160	320	198	129	0.806
	400	201	159	0.994

equipment. Here, we marked the phantom for the sake of good reproducibility. To measure the ESDs, both the GafchromicTM film and nanoDotTM OSL dosimeters were placed on the water phantom as shown in Fig. 2. The GafchromicTM film was cut into 10 mm-wide by 100 mm-long pieces, which were pasted on the back side of a paper sheet. The nanoDotTM OSL dosimeters were lined up on the front side of the sheet; the dimensions of the dosimeters matched those of the pieces of GafchromicTM film. Owing to the precise experimental setup, we could easily identify the relative positions in which the nanoDotTM OSL dosimeters were set.

Table 1 summarizes the irradiation conditions. The relationships between the PF and number of detector rows used in the experiment were as follows: PF = 0.688, 0.938, 1.348 for 16 rows; PF = 0.656, 0.844, 1.406 for 32 rows; PF = 0.641, 0.828, 1.484 for 64 rows; PF = 0.637, 0.813, 1.388 for 80 rows; PF = 0.810, 1.390 for 100 rows; and PF = 0.806, 0.994 for 160 rows. We set the tube currents to obtain similar effective doses of approximately 200 mAs (= tube current \times rotation time/pitch factor). The following parameters were fixed: tube voltage of 120 kV, rotation time of 0.5 s, large field of view (FOV = 400 mm in diameter), and irradiation length of 450 mm, the same as the length of the water phantom. When a prescan was performed to determine the irradiation size of the water phantom, we did not place the GafchromicTM film and nanoDotTM OSL dosimeters on the phantom. After the prescan, both the GafchromicTM film and nanoDotTM OSL dosimeters were placed on the water phantom, and the examination scan was performed. We then analyzed the ESDs measured using the GafchromicTM film and

nanoDotTM OSL dosimeters as functions of the PF and number of detector rows.

In addition, we performed an experiment for visualizing the ESD distribution on a human body phantom (PBU-60, Kyoto Kagaku, Ltd., Kyoto, Japan) using the nanoDotTM OSL dosimeters in clinical settings. Figure 3 shows a photograph of the experiment. The nanoDotTM OSL dosimeters were attached to the body phantom at intervals 2 cm in width and 5 cm in length; 90 dosimeters were laid out on a region with a width of 18 cm (nine dosimeters) and a length of 50 cm (10 dosimeters). The irradiation condition of the general scan protocol from chest to pelvis was used. The conditions were as follows: tube voltage of 120 kV, 80 rows of detectors, detector size of 0.5 mm, PF of 0.814, large FOV, and effective tube current time product of 166 mAs. Here, experiments were performed in the CT scan mode with and without an adaptive iterative dose reduction (Volume EC+ AIDR3D) system proposed by Toshiba [25, 26].

3 Results

3.1 ESDs on the water phantom

Figure 4 shows the ESD distributions under all the conditions in the CT scans; (a), (b), (c), (d), (e), and (f) show the results for 16, 32, 64, 80, 100, and 160 rows, respectively. In these figures, the horizontal axis represents the relative dosimeter position. The vertical axis represents the ESDs. Values measured using the GafchromicTM film and nanoDotTM OSL dosimeters are represented by small open

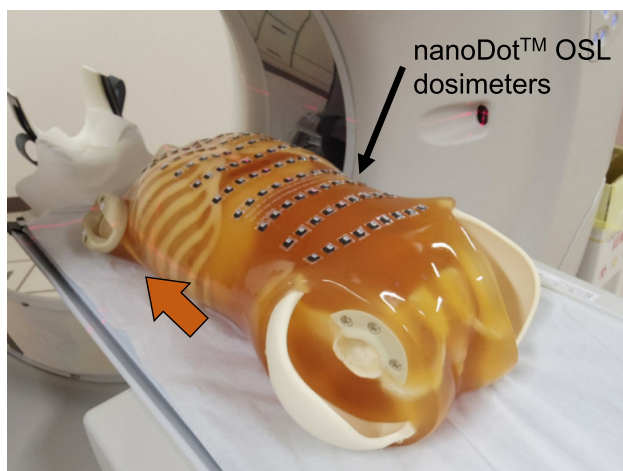


Fig. 3 Photograph of the experiment in which the ESD distribution of the body phantom was measured using nanoDot™ OSL dosimeters

circles and large solid circles, respectively. The uncertainties of the nanoDot™ OSL dosimeters from Eq. (2) were applied. For all the irradiation conditions, the ESDs of the nanoDot™ OSL dosimeter were in good agreement with those measured using the Gafchromic™ film, within the margin of their uncertainties. The broken lines represent the mean value of the ESD distribution measured using the Gafchromic™ film.

The mean value is important in this study for the evaluation of the precision of the nanoDot™ OSL dosimeters during the CT scans. To perform the evaluation, the differences between the mean values of the ESD distribution and the ESDs measured using the nanoDot™ OSL dosimeters were calculated, and they are plotted in Fig. 5. Here, we define the precision of the nanoDot™ OSL dosimeters as the maximum difference; the levels (and numerical values) are displayed as dashed lines in the figure. Under most irradiation conditions, the accuracies were estimated to be below 25 %, except for the following three conditions: 64 rows with PF = 1.484 (Fig. 4c-3), 80 rows with PF = 1.388 9 (Fig. 4d-3), and 100 rows with PF = 1.390 (Fig. 4e-2).

3.2 Visualization of ESD distributions using the human body phantom

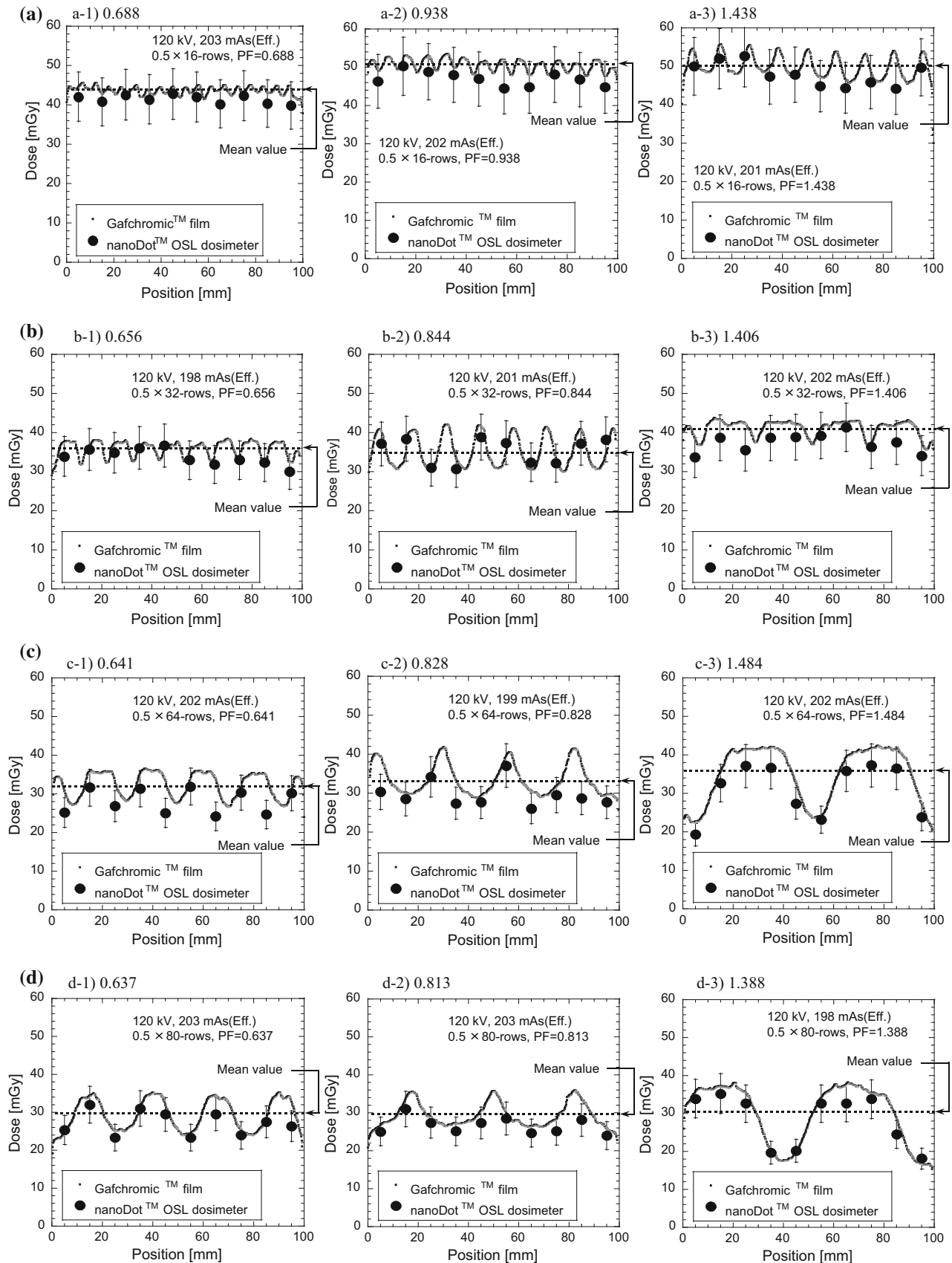
Figure 6 shows the results of the visualization of the ESD measurements when the nanoDot™ OSL dosimeters were placed on the human body phantom. Figure 6a shows the CT image derived by the CT scan; we can observe the nanoDot™ OSL dosimeters on the surface of the human body phantom. Figure 6b shows the two-dimensional distribution of the measured ESDs in a normal scan, and Fig. 6c shows the results obtained using the dose reduction system. Higher ESDs are shown in red and lower ones in

yellow. A comparison of b and c clearly reveals that the dose reduction system is effective in the lung field. Figure 6d, e shows the cross-sectional CT images with the lung window corresponding to the positions identified by arrows in b and c, respectively. In these images, the positions of the nanoDot™ OSL dosimeters can be easily found. Figure 6f, g shows the cross-sectional CT images with the mediastinal window for the same positions as in d and e, respectively. In contrast to d and e, in the images in f and g, it is difficult to identify the positions at which the nanoDot™ OSL dosimeters were attached.

4 Discussion

In this study, we tried to apply the small OSL dosimeter, nanoDot™, to measure the ESD during CT examinations. In CT scans, irradiated X-rays are collimated into a slit beam; therefore, the measured counts of the dosimeter irradiated by the slit beams undergo intricate fluctuations in response to the chosen PF and the number of detector rows. Although the outer dimensions of the nanoDot™ OSL dosimeter result in convenient measurements when they are placed on patients, this placement may cause reduced stability. To use the nanoDot™ OSL dosimeter in clinical settings, the uncertainties of the ESDs and their limitations were evaluated as follows.

To estimate the uncertainties of the ESDs measured using the nanoDot™ OSL dosimeters, measurements were also performed using the Gafchromic™ film and a water phantom. The ESDs measured under all the scanning conditions using the nanoDot™ OSL dosimeters were consistent with those measured using Gafchromic™ film, as shown in Fig. 4. These results are important, because the dose calibration methods for the nanoDot™ OSL dosimeters and Gafchromic™ film are completely different in this study. The nanoDot™ OSL dosimeters were calibrated by the practical method we proposed [22] on the basis of air kerma measurements with X-rays of HVL = 3.0 mmAl (83 kV), whereas the Gafchromic™ films were calibrated under X-rays with a quality of HVL = 7.2 mmAl (120 kV). In our method for evaluating the nanoDot™ OSL dosimeters, the energy and angular dependences and the characteristics of different dosimeters were considered to be within an uncertainty of 15 %. The results indicate that these previous findings can be applied to ESD measurements during CT scans. Gafchromic™ film is widely used for evaluating the ESD distributions during CT scans [12, 27]. For cases in which precise dose distributions should be measured, it may be a suitable tool. In contrast, for convenient evaluation of doses, the nanoDot™ OSL dosimeter also becomes a valuable tool. In the near future, medical diagnoses will become more



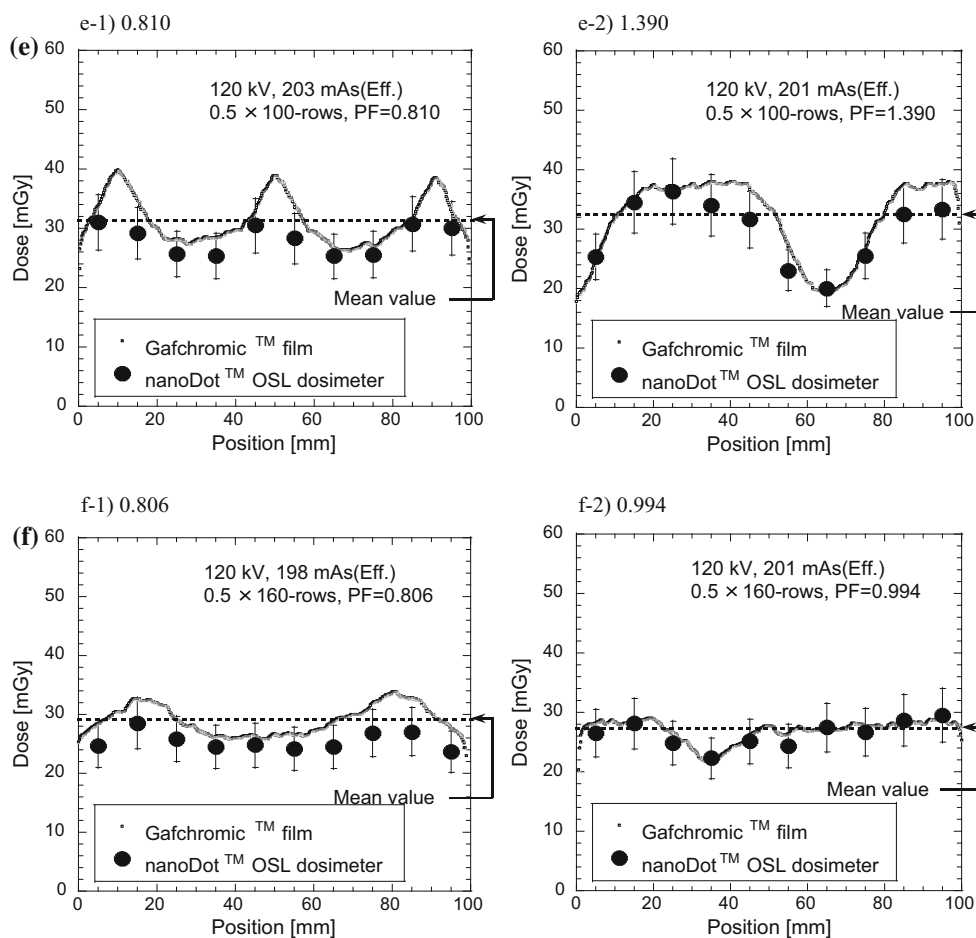
◀ **Fig. 4** Comparison of the ESDs measured using the nanoDot™ OSL dosimeter (*large solid circles*) and Gafchromic™ film (*small open circles*). Dashed line indicates a mean value measured using the Gafchromic™ film. The values measured using the nanoDot™ OSL dosimeters are in good agreement with those obtained using the Gafchromic™ film

complicated because of the use of multimodalities; patients will have to undergo examinations involving not only a single CT scan, but also plain X-rays, dual-energy CT scans, and so on. Medical staff will have to evaluate the actual overall doses administered to patients. Our method using the nanoDot™ OSL dosimeters can be used to evaluate the doses without the need to gather information concerning the energy and angular dependences, because our method includes the uncertainty of ignoring these effects. Thus, our method will be valuable for the management of actual patient doses.

Here, using the ESD distributions measured using the Gafchromic™ films in Fig. 4 as the reference ESD, the accuracies and limitations of those measured using the nanoDot™ OSL dosimeters were evaluated. The differences of the ESDs measured using dosimeters from the mean value of the reference ESD are represented in Fig. 5;

the accuracies of the nanoDot™ OSL dosimeters are defined as these differences. Relatively high accuracies (small differences from the mean values) were derived when PFs close to 1.000 were used. Under this condition, the nanoDot™ OSL dosimeters were uniformly irradiated; therefore, the observed deviations became smaller. On the other hand, when the PFs were not close to 1.000, the accuracies decreased rapidly. In particular, the following three conditions showed less than favorable results: accuracy of 47 % for PF = 1.484 (64 rows), 41 % for PF = 1.388 (80 rows), and 38 % for PF = 1.390 (100 rows). These findings can be explained as follows. When the helical CT scan was performed using 64 rows and a PF of 1.484, the irradiation area became 32 mm (= 64[*row*] × 0.5[mm/*row*]) in the direction of the long axis, and no irradiation area of 15.5 mm [= 32[mm] × (1.484 – 1.000)] appeared at the isocenter. As a result, some dosimeters were irradiated only by scattered X-rays (no direct X-rays), and lower ESDs were observed compared to those of the other dosimeters irradiated by both direct and scattered X-rays. From these results, we proposed that the nanoDot™ OSL dosimeter should not be used for PFs of 1.484 for 64 rows, 1.388 for

Fig. 4 continued



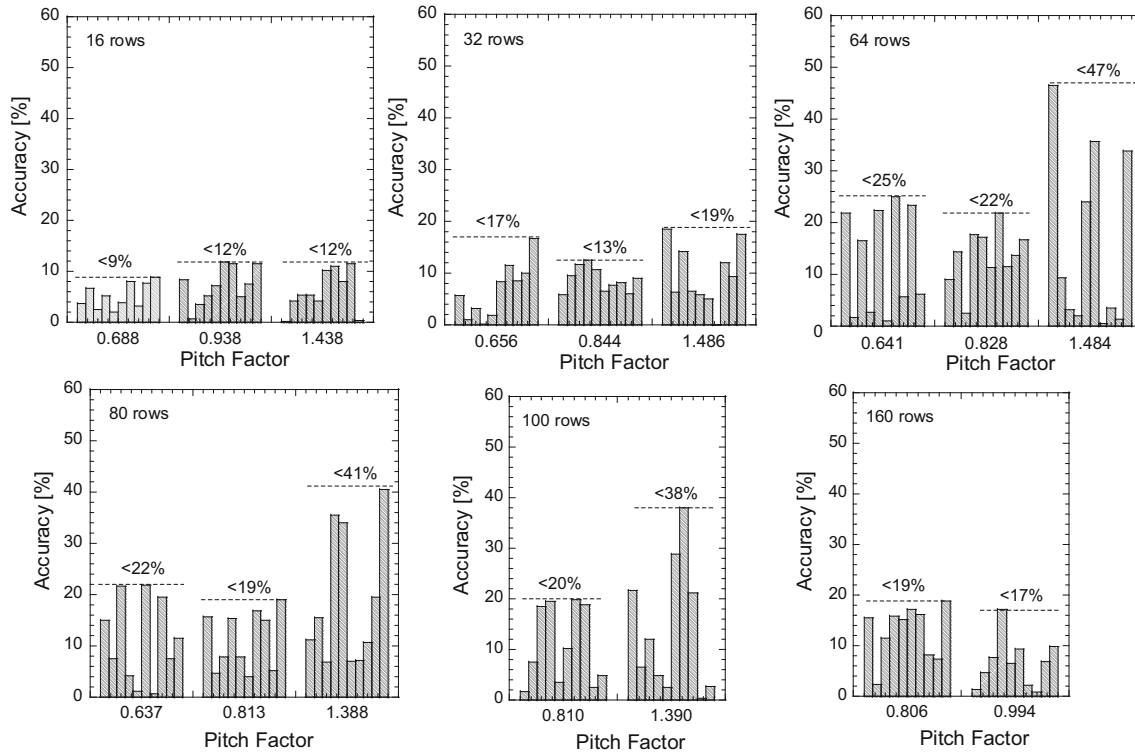


Fig. 5 Evaluation of the accuracy of our method, in which the nanoDot™ OSL dosimeter was used for CT scans. For each irradiation condition, absolute values of the differences for ten dosimeters are plotted

80 rows, and 1.390 for 100 rows. Under the conditions that we adopt, the maximum uncertainty is found to be 25 % (PF = 0.641, 64 rows). Then, we proposed that an additional uncertainty ($\sigma_{\text{sys,CT}}$) of 25 % will be considered in estimating the total uncertainty ($\sigma_{\text{t,CT}}$) of the CT scan, as follows:

$$\sigma_{\text{t,CT}} = \sqrt{\sigma_{\text{sta}}^2 + \sigma_{\text{sys}}^2 + \sigma_{\text{sys,CT}}^2}. \quad (4)$$

In typical CT examinations, σ_{sta} is less than 1 %, σ_{sys} is 15 %, and $\sigma_{\text{sys,CT}}$ is 25 %; therefore, $\sigma_{\text{t,CT}}$ becomes 30 %. Although an accuracy of 30 % is not good, the nanoDot™ OSL dosimeter is expected to be useful for making direct ESD measurements of patients undergoing CT examinations. Note that this estimation is limited to experiments using a 320-row CT scanner manufactured by Toshiba. For CT scanners of other manufacturers, the applicability limit of the present results is unclear. In the next paragraph, we describe the effective clinical applications for measuring patient doses during CT scans.

For clinical application, it is important that nanoDot™ OSL dosimeters, when placed on the human body, do not interfere with the medical images. Metals (high atomic number materials) are known causes of artifacts in images obtained in CT scans. The nanoDot™ OSL dosimeter consists of relatively low atomic number materials; the detector region is 78.4 % Al_2O_3 and 21.6 % polyester with

a density of 1.41 g/cm^3 and a thickness of 200 μm . The cover is composed of polyester with a density of 1.18 g/cm^3 and a thickness of less than 2 mm [20]. These values are negligibly small compared to those of the human body. Therefore, it is expected that no artifacts will be present in the images. In fact, we could not detect additional artifacts in the cross-sectional views in Fig. 6d–g. The results represent a valuable verification to support the application of the dosimeter in clinical applications. In Fig. 6b, c, the distributions of the ESDs are clearly observed. These images are useful for the evaluation of doses, for education, and so on. In the near future, we plan to measure the actual ESDs of patients using the nanoDot™ OSL dosimeter, and the proper position to place the dosimeter is now under consideration.

Finally, we discuss the future prospects for dose measurement using the nanoDot™ OSL dosimeter. In all the X-ray examinations performed in clinics, the most important dose is the effective dose administered to the organs of the human body. By considering radiation-weighted factors [28] concerning the organs of interest, an effective dose can be derived. During a CT examination, the effective dose is estimated from the dose-length product (DLP) using conversion coefficients reported by Christner et al. [29]. Moreover, the DLP is calculated from the volume CTDI, CTDI_{vol} , and the irradiated length during the CT

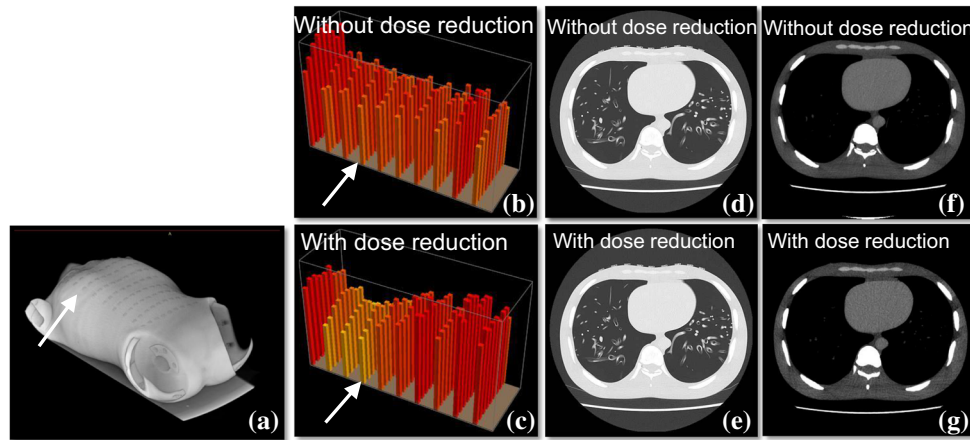


Fig. 6 Demonstration of two-dimensional ESD distributions on the body phantom. *Red* and *yellow bars* represent high and low values, respectively. **a** CT image, **b** ESD distribution of the normal scan, and **c** ESD distribution using the dose reduction process proposed by Toshiba Ltd. (Volume EC+ AIDR3D). **d**, **e** Cross-sectional CT

images with lung window under irradiation conditions with and without the dose reduction process, respectively. **f**, **g** Cross-sectional CT images with mediastinal window under irradiation conditions with and without the dose reduction process, respectively

scans. The entrance skin dose was another important dose to be evaluated, because one can measure the dose easily compared to the $CTDI_{vol}$. A relationship between the $CTDI_{vol}$ and the entrance skin dose was reported elsewhere [13]. The dose measured using GafchromicTM film was the ESD; therefore, we converted the ESD to the entrance skin dose using the following equation:

$$\begin{aligned} \text{Entrance skin dose} &= \text{ESD} \times \frac{(\mu_{en}/\rho)_{\text{soft-tissue}}}{(\mu_{en}/\rho)_{\text{air}}} \\ &= \text{ESD} \times 1.064. \end{aligned} \quad (5)$$

In this calculation, we assumed that the effective energy of CT X-rays was approximately 50 keV, and the corresponding mass energy absorption coefficients were from Ref. [30]. However, we did not distinguish a difference between the entrance skin dose and the ESD for the measured value using the nanoDotTM OSL dosimeter, because the experimental uncertainty of the measured value included the differences. Then, as shown in Fig. 7, we preliminarily examined the relationship between the $CTDI_{vol}$ and entrance skin dose using the data derived in the present experiments. The *y* axis shows the entrance skin doses, where the solid and open symbols represent the mean values of the nanoDotTM OSL dosimeters and GafchromicTM film, respectively, and the *x* axis represents the $CTDI_{vol}$, which was determined in the CT equipment. A good correlation between the $CTDI_{vol}$ and the entrance skin doses was observed. The solid line represents the relationship proposed previously by Westra et al. [13]. Our data are in good agreement with their relationship. From this fact, one may conclude that the entrance skin dose measurement is an indirect method for making effective dose evaluations for the whole body. Our method using the

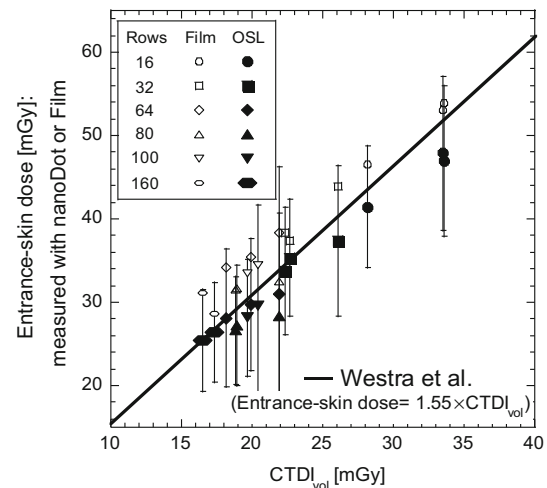


Fig. 7 Relationship between $CTDI_{vol}$ and entrance skin dose. The entrance skin doses were derived from the measured values using the nanoDotTM OSL dosimeters (*solid symbols*) and GafchromicTM film (*open symbols*). The $CTDI_{vol}$ was calculated using the software installed in the CT computer

nanoDotTM OSL dosimeter is convenient; therefore, everyone can apply our results for improving clinical CT examinations.

5 Conclusion

In conclusion, we evaluated the ability to measure the ESD of a patient using a small OSL dosimeter called the nanoDotTM during CT scans. By comparing ESDs measured using the nanoDotTM OSL dosimeter and GafchromicTM film, the accuracy of the CT scans was found to be

25 % for most irradiation conditions. Considering this result in combination with previous research on the evaluation of the energy and angular dependences, and variability of the individual nanoDot™ OSL dosimeters, we concluded that the nanoDot™ OSL dosimeter can measure the ESD of patients with total uncertainties of 30 %. Our results show the possibility of obtaining an extremely large uncertainty when nanoDot™ OSL dosimeters are used under the following conditions: PFs of 1.484 (64 rows), 1.388 (80 rows), and 1.390 (100 rows). Therefore, we suggest that the dosimeter should be used under a PF of less than 1.000. In addition, we demonstrated visualization of the ESD distributions with and without the dose reduction protocol proposed by Toshiba. We also verified that there were no additional artifacts in the cross-sectional CT images when the nanoDot™ OSL dosimeter was placed on patients. These results can help us manage the exposure doses of patients.

Acknowledgments This work was supported by JSPS KAKENHI Grant Number 15K19205.

Compliance with ethical standards

Conflict of interest T Okazaki, T. Hashizume, and I. Kobayashi are employees of Nagase Landauer Ltd. and collaborating researchers.

References

- Gonzalez AB, Darby S. Risk of cancer from diagnostic X-ray: estimates for the UK and 14 other countries. *Lancet*. 2004;363:345–51. doi:10.1016/S0140-6736(04)15433-0.
- Uffmann M, Schaefer-Prokop C. Digital radiography: the balance between image quality and required radiation dose. *Eur J Radiol*. 2009;72:202–8. doi:10.1016/j.ejrad.2009.05.060.
- Gardner SJ, Studenski MT, Giaddui T, et al. Investigation into image quality and dose for different patient geometries with multiple cone-beam CT systems. *Med Phys*. 2014;41(3):031908. doi:10.1118/1.4865788.
- Goldman LW. Principles of CT: radiation dose and image quality. *J Nucl Med Technol*. 2007;35(4):213–25. doi:10.2967/jnmt.106.037846.
- Mathews JD, Forsythe AV, Brady Z, et al. Cancer risk in 680,000 people exposed to computed tomography scans in childhood or adolescence: data linkage study of 11 million Australians. *BMJ*. 2013;346:f2360. doi:10.1136/bmj.f2360.
- McCullough CH, Leng S, Yu L, et al. CT dose index and patient dose: they are not the same thing. *Radiol*. 2011;259:311–6. doi:10.1148/radiol.11101800.
- Koyama S, Aoyama T, Oda N, et al. Radiation dose evaluation in tomosynthesis and C-arm cone-beam CT examinations with an anthropomorphic phantom. *Med Phys*. 2010;. doi:10.1118/1.3465045.
- McDermott A, White RA, Mc-Nitt-Gray M, et al. Pediatric organ dose measurements in axial and helical multislice CT. *Med Phys*. 2009;36(5):1494–9. doi:10.1118/1.3101817.
- Tsalatoutas IA, Epistatou A, Nikolettopoulos S, et al. Measuring skin dose in CT examinations under complex geometries: instruments, methods and considerations. *Physica Med*. 2015;31:1005–14. doi:10.1016/j.ejmp.2015.08.001.
- Tappouni R, Mathers B. Scan quality and entrance skin dose in thoracic CT: a comparison between bismuth breast shield and posteriorly centered partial CT scans. *ISRN Radiol*. 2013;. doi:10.5402/2013/457396 (article ID 457396).
- Duan X, Wang J, Christner JA, et al. Dose reduction to anterior surfaces with organ-based tube-current modulation: evaluation of performance in a phantom study. *Am J Roentgenol*. 2011;197:689–95. doi:10.2214/AJR.10.6061.
- Tominaga M, Kawata Y, Niki N, et al. Measurements of multi-detector CT surface dose distributions using a film dosimeter and chest phantom. *Med Phys*. 2011;38:2467. doi:10.1118/1.3570769.
- Westra SJ, Li X, Gulati K, et al. Entrance skin dosimetry and size-specific dose estimate from pediatric chest CTA. *J Cardiovasc Comput Tomogr*. 2014;8:97–107. doi:10.1016/j.jcct.2013.08.002.
- Ramac JP, Knezevic Z, Hebrang A, et al. Radiation dose reduction by using low dose CT protocol of thorax. *Radiat Meas*. 2013;55:46–50. doi:10.1016/j.radmeas.2012.07.012.
- Cordasco C, Portelli M, Miliati A, et al. Low-dose protocol of the spiral CT in orthodontics: comparative evaluation of entrance skin dose with traditional X-ray techniques. *Prog Orthod*. 2013;14:24. doi:10.1186/2196-1042-14-24.
- Takegami K, Hayashi H, Okino H, et al. Estimation of identification limit for a small-type OSL dosimeter on the medical images by measurement of X-ray spectra. *Radiol Phys Technol*. 2016;. doi:10.1007/s12194-016-0362-5 (in press).
- Takegami K, Hayashi H, Nakagawa K, et al. Measurement method of an exposed dose using the nanoDot dosimeter. *Eur Con Radiol (EPOS)*. 2015;. doi:10.1594/ecr2015/C-0218.
- Hayashi H, Nakagawa K, Okino H, et al. High accuracy measurements by consecutive readings of OSL dosimeter. *Med Imaging Inf Sci*. 2014;31(2):28–34. doi:10.11318/mii.31.28.
- Nakagawa K, Hayashi H, Takegami K, et al. Fabrication of annealing equipment for optically stimulated luminescence (OSL) dosimeter. *Jpn J Radiol Technol*. 2014;70(10):1135–42. doi:10.6009/jjrt.2014_JSRT_70.10.1135.
- Hayashi H, Takegami K, Okino H, et al. Procedure to measure angular dependences of personal dosimeters by means of diagnostic X-ray equipment. *Med Imaging Inf Sci*. 2015;32(1):8–14. doi:10.11318/mii.32.8.
- Takegami K, Hayashi H, Okino H, et al. Energy dependence measurement of small-type optically stimulated luminescence (OSL) dosimeter by means of characteristic X-rays induced with general diagnostic X-ray equipment. *Radiol Phys Technol*. 2016;9:99–108. doi:10.1007/s12194-015-0339-9.
- Takegami K, Hayashi H, Okino H, et al. Practical calibration curve of small-type optically stimulated luminescence (OSL) dosimeter for evaluation of entrance-skin dose in the diagnostic X-ray. *Radiol Phys Technol*. 2015;8:286–94. doi:10.1007/s12194-015-0318-1.
- Giaddui T, Cui Y, Galvin J, et al. Comparative dose evaluations between XVI and OBI cone beam CT systems using Gafchromic™ XRQA2 films and nanoDot optical stimulated luminescence dosimeters. *Med Phys*. 2013;40:062102. doi:10.1118/1.4803466.
- Tomic N, Devic S, DeBlois F, et al. Reference radiochromic film dosimetry in kilovoltage photon beams during CBCT image acquisition. *Med Phys*. 2010;37. doi:10.1118/1.3302140.
- Yamashiro T, Miyara T, Honda O, et al. Adaptive iterative dose reduction Using three dimensional processing (AIDR 3D) improves chest CT image quality and reduces radiation exposure. *PLoS One*. 2014;9(8):e105735. doi:10.1371/journal.pone.0105735.
- Yamada Y, Jinzaki M, Hosokawa T, et al. Dose reduction in chest CT: comparison of the adaptive iterative dose reduction 3D,

- adaptive iterative dose reduction, and filtered back projection reconstruction techniques. *Eur J Radiol.* 2012;81:4185–95. doi:[10.1016/j.ejrad.2012.07.013](https://doi.org/10.1016/j.ejrad.2012.07.013).
27. D'Alessio D, Giliberti C, Soriani A, et al. Dose evaluation for skin and organ in hepatocellular carcinoma during angiographic procedure. *J Exp Clin Cancer Res.* 2013;32:81. doi:[10.1186/1756-9966-32-81](https://doi.org/10.1186/1756-9966-32-81).
28. Sabarudin A, Sun Z. Radiation dose measurement in coronary CT angiography. *World J Cardiol.* 2013;5(12):459–64. doi:[10.4330/wjc.v5.i12.459](https://doi.org/10.4330/wjc.v5.i12.459).
29. Christner JA, Kofler JM, McCollough CH. Estimating effective dose for CT using dose-length product compared with using organ doses: consequences of adopting international commission on radiological protection publication 103 or dual-energy scanning. *Am J Rentgenol.* 2010;194:881–9. doi:[10.2214/AJR.09.3462](https://doi.org/10.2214/AJR.09.3462).
30. Hubbell JH. Photon mass attenuation and energy-absorption coefficients. *Int J Appl Radiat Isotopes.* 1982;33(11):1269–90. doi:[10.1016/0020-708X\(82\)90248-4](https://doi.org/10.1016/0020-708X(82)90248-4).